Thalidomide Radiosensitizes Tumors through Early Changes in the Tumor Microenvironment

Réginald Ansiaux,[1] Christine Baudelet,[1,2] Bénédicte F. Jordan,[1,2] Nelson Beghein,[1,2] Pierre Sonveaux,[3] Julie De Wever,[3] Philippe Martinive,[3] Vincent Grégoire,[4] Olivier Feron,[3] and Bernard Gallez[1,2]

Laboratories of [1]Biomedical Magnetic Resonance, [2]Medicinal Chemistry and Radiopharmacy, and [3]Pharmacology and Therapeutics and [4]Radiobiology and Radioprotection Unit, Université Catholique de Louvain, Brussels, Belgium

ABSTRACT

Purpose: **The aim of this work was to study changes in the tumor microenvironment early after an antiangiogenic treatment using thalidomide (a promising angiogenesis inhibitor in a variety of cancers), with special focus on a possible "normalization" of the tumor vasculature that could be exploited to improve radiotherapy.**

Experimental Design: **Tumor oxygenation, perfusion, permeability, interstitial fluid pressure (IFP), and radiation sensitivity were studied in an FSAII tumor model. Mice were treated by daily i.p. injection of thalidomide at a dose of 200 mg/kg. Measurements of the partial pressure of oxygen (pO_2) were carried out using electron paramagnetic resonance oximetry. Three complementary techniques were used to assess the blood flow inside the tumor: dynamic contrast-enhanced magnetic resonance imaging, Patent Blue staining, and laser Doppler imaging. IFP was measured by a "wick-in-needle" technique.**

Results: **Our results show that thalidomide induces tumor reoxygenation within 2 days. This reoxygenation is correlated with a reduction in IFP and an increase in perfusion. These changes can be attributed to extensive vascular remodeling that we observed using CD31 labeling.**

Conclusions: **In summary, the microenvironmental changes induced by thalidomide were sufficient to radiosensitize tumors. The fact that thalidomide radiosensitization was not observed *in vitro*, and that *in vivo* radiosensitization occurred in a narrow time window, lead us to believe that initial vascular normalization by thalidomide accounts for tumor radiosensitization.**

Received 7/20/04; revised 9/30/04; accepted 10/6/04.

Grant support: Belgian National Fund for Scientific Research grant 7.4503.02, the Fonds Joseph Maisin, and the "Actions de Recherches Concertées—Communauté francaise de Belgique."

The costs of publication of this article were defrayed in part by the payment of page charges. This article must therefore be hereby marked *advertisement* in accordance with 18 U.S.C. Section 1734 solely to indicate this fact.

Requests for reprints: Bernard Gallez, CMFA/REMA Units, Université Catholique de Louvain, Avenue E. Mounier 73.40, B-1200 Brussels, Belgium. Phone: 32-2-7642792; Fax: 32-2-7642790; E-mail: Gallez@cmfa.ucl.ac.be.

©2005 American Association for Cancer Research.

INTRODUCTION

During tumor growth, the formation of a new tumor vascular network from preexisting blood vessels (angiogenesis) is essential for delivery of oxygen and nutrients to the entire tumor mass, allowing expansion (1, 2). However, tumor neovessels remain structurally and functionally abnormal (1–3). Most of them are dilated, tortuous with extensive fenestrations, branchings, and arteriovenous shunts. This abnormal organization reduces therapeutic effectiveness (4): blood flow in these vessels is highly variable (4, 5) and excessive vascular leakiness further accounts for high tumor interstitial fluid pressure (IFP), eventually equalizing the intravascular pressure (4). Such tumor peculiarities prevent the uniform delivery of circulating chemotherapeutic agents and oxygen (a radiotherapy enhancer).

Antiangiogenic therapies have been proposed to gradually deprive a tumor of its blood supply (6). Although such approaches have had attractive results in animal models, they have been disappointing in clinical trials. This has prompted efforts to combine antiangiogenic treatments with other treatment modalities. The combination of antiangiogenic agents with radiotherapy has been suggested because it should target both the tumor cells and the endothelial cells. However, this strategy also seems counterintuitive: it is well established that conventional radiotherapy requires sufficient tumor oxygenation to avoid radioresistance, and antiangiogenic therapies should lead to a decrease in oxygen, thereby lowering radiosensitivity. A possible explanation for a potential synergistic effect is that the administration of antiangiogenic agent could first prune the immature and inefficient blood vessels and consequently result in an early "normalization" of the tumor vasculature (7). This hypothesis is further supported by studies that have blocked the signaling of vascular endothelial growth factor (a potent proangiogenic factor), which resulted in apoptosis of endothelial cells and a decrease in vessel diameter, density, and permeability (8–10). This consequently leads to a decrease in the IFP and an increase in tumor oxygen partial pressure (pO_2; refs. 8, 11, 12).

The efficacy of combining antiangiogenic therapy with chemotherapy (13, 14) or radiotherapy (12, 15–17) has been recently reported. However, the net effect of antiangiogenic treatment on the evolution of the tumor microenvironment (including parameters such as pO_2, perfusion, IFP, and their evolution with the time after treatment) has been neglected in many studies.

The purpose of the present study is to monitor the evolution of the tumor microenvironment early after an antiangiogenic treatment and to determine if there exists an optimal time window for cotreatment with radiotherapy. The antiangiogenic agent used in our study was thalidomide (one of the most studied antiangiogenic agents in clinical trials). Thalidomide was shown to inhibit basic fibroblast growth factor (18) as well as vascular endothelial growth factor (19, 20), two promoters of angiogenesis. A direct antitumor effect has been shown in rabbits (21) and humans (22).

In this work, we report a transient increase in tumor oxygenation 2 days after the beginning of the treatment, paralleling changes in tumor perfusion and interstitial pressure. At that time, tumors were radiosensitized. Such radiosensitization was absent when radiotherapy was delivered earlier or later, thereby emphasizing the need to monitor the tumor microenvironment when combining antiangiogenic treatments with radiotherapy.

MATERIALS AND METHODS

Mice and Tumors

Syngeneic FSAII fibrosarcoma tumor cells (23) were injected i.m. into the thigh of male C3H/HeOuJIco mice. Tumors were measured daily with an electronic caliper. Thalidomide or DMSO treatment (control) was started when tumors reached a diameter of 8.0 ± 1.0 mm. Racemic thalidomide (Sigma-Aldrich, Bornem, Belgium) was dissolved in DMSO and was given daily via 100-μL i.p. injection (200 mg/kg). For all experiments, tumor-bearing mice were anesthetized using isoflurane (2.5% for induction, 1% for maintenance). All animal experiments were done in accordance with national animal care regulations.

Tumor Oxygenation

Electronic paramagnetic resonance (EPR) oximetry (using charcoal as oxygen-sensitive probe) was used to evaluate tumor oxygenation changes after thalidomide treatment using a protocol described previously (24–26). EPR spectra were recorded using an EPR spectrometer (Magnettech, Berlin, Germany) with a low-frequency microwave bridge operating at 1.2 GHz and an extended loop resonator. Mice were given injections in the center of the tumor 2 days before measurement using the charcoal suspension (100 mg/mL, 50 μL injected, 1- to 25-μm particle size). The localized EPR measurements correspond to an average of pO_2 values in a volume of ~10 mm^3 (25). To avoid any acute effect of the treatment, data acquisition was made before the first injection of thalidomide or DMSO and then on a daily basis for 1 week.

Flow Measurements

Patent Blue Staining. Patent Blue (Sigma-Aldrich) was used to obtain a rough estimate of the tumor perfusion (27) after 2 days of treatment with thalidomide or vehicle. This technique involves the injection of 200 μL of Patent Blue (1.25%) solution into the tail vein of the mice. After 1 minute, a uniform distribution of the staining through the body was obtained and mice were sacrificed. Tumors were carefully excised and cut into size-matched halves. Pictures of each tumor cross section were taken with a digital camera. To compare the stained versus unstained area, an in-house program running on Interactive Data Language (Research Systems Inc., Boulder, CO) was developed. For each tumor, a region of interest (stained area) was defined on the two pictures and the percentage of stained area of the whole cross section was determined. The mean of the percentages of the two pictures was then calculated and was used as an indicator of tumor perfusion.

Laser Doppler Imaging. Superficial tumor perfusion was assessed using a laser Doppler imager (Moor Instruments, Millwey, United Kingdom) after 2 days of treatment with thalidomide or vehicle. The skin was depilated the day before measurement. To minimize variations in temperature, mice were placed on a heating pad (37°C). The laser beam moved step by step in a rectangular pattern over the skin surface. The light penetrated the skin to a depth of 2 to 3 mm. In the presence of moving red blood cells in nutritional capillaries, arterioles, and venules, a fraction of the light is Doppler shifted, detected, and converted into a computerized, color-coded image. One measurement before treatment and one after 2 days of treatment were done with each mouse. Using image analysis software (Laser Doppler Perfusion measure, V3.0.8, Moor Instruments), mean flux values, representing the tumor perfusion, were calculated from the relative flux units.

Dynamic Contrast-Enhanced Magnetic Resonance Imaging. This technique was used to assess changes in tumor perfusion and tracer penetration after 2 days of thalidomide treatment. Magnetic resonance imaging (MRI) was done with a 4.7-T (200 MHz, ^1H) 40-cm inner diameter bore system (Bruker Biospec, Ettlingen, Germany). T2-weighted anatomic images were acquired using a fast spin-echo sequence (repetition time = 3 seconds, effective echo time = 63 milliseconds]. A single, 1.3-mm-thick slice passing through the tumor center was prescribed. A birdcage radiofrequency coil with an inner diameter of 70 mm was used for radiofrequency transmission and reception. For dynamic contrast-enhanced MRI (DCE-MRI) studies, two slices were selected: one was centered on the kidneys and the other was positioned on the tumor. T_1-weighted gradient-recalled echo images were obtained with the following parameters: repetition time = 40 milliseconds, effective echo time = 4.9 milliseconds, 1.6-mm slice thickness, flip angle = 90°, matrix = 64 × 64, field of view = 6 cm, 25-kHz receiver bandwidth, resulting in an acquisition time of 2.56 seconds per scan. The DCE study was done using the following protocol. First, a set of 200 scans (8 minutes 32 seconds) was done dynamically. After the first 12 of these images had been acquired (for the baseline), P792 (Vistarem, Laboratoire Guerbet, Aulnay sous Bois, France) was given i.v. within 2 seconds (42 μmol/kg, 50 μL/30 g mouse). P792 (molecular weight, 6.47 kDa) is a monogadolinium macrocyclic compound based on a gadolinium-1,4,7,10-tetra-azacylododecane *N,N′,N′,N′′′*-tetraacetic acid structure substituted by hydrophilic (dextran) arms. In this way, the signal intensity curve was therefore sampled to track the fast increase in tissue enhancement for viable tumor after the bolus injection. A second set of 60 images was then acquired over 1 hour to monitor the washout of the contrast agent. A calibration curve was generated with a Sephadex gel bead phantom (G-100, Pharmacia Fine Chemicals, Uppsala, Sweden) to convert signal enhancement into contrast agent concentration.

Kinetics Analysis. DCE-MRI raw data were zero-filled and two-dimensional Fourier transformed, resulting in an in-plane resolution of 128 × 128. An operator-defined region of interest encompassing the tumor was analyzed on a voxel-by-voxel basis to obtain parametric maps. A power spectrum analysis (28) was done to identify voxels with statistically significant variations in signal intensity. Among these voxels,

only those for which the typical signal enhancement curve was observed were selected for the pharmacokinetic analysis (i.e., voxels showing either linear or no increase of signal intensity were discarded). This was done using a cluster analysis (28). Thereafter, the relative signal intensity enhancements (S/S0) were converted into P792 concentration (in millimoles per liter) using an equation generated by the *in vitro* calibration at 4.7T. The tumor P792 concentration versus time curves were analyzed by a two-compartment bidirectional pharmacokinetics model (29). The monoexponential decay rate of the contrast agent in the blood stream was estimated from the enhancement kinetics in the renal cortex. The concentration of the contrast agent in tumor contained contributions from the vascular and extravascular compartments and was fitted by using a four-parameter model: D_0 (mmol/L), D_1 (mmol/L/min), K_2 (min^{-1}), and t_0 (min).

D_0 is proportional to the plasma volume fraction and is related to the initial slope of the concentration-time curve:

$$D_0 = V_p A_0$$

where V_p is the plasma volume fraction and A_0 is the maximum plasma P792 concentration.

D_1 is proportional to the rate of tracer accumulation in the interstitial space, and it determines the peak enhancement. If the blood supply is sufficient, D_1 will depend on the permeability, total capillary surface area, and interstitial pressure.

$$D_1 = V_e A_0 K_1$$

where V_e is the volume fraction of the extravascular extracellular space and K_1 is the leakage rate.

K_2 is the fractional rate of efflux from the interstitial space back to the blood stream. t_0 is the time to the maximum tracer plasma concentration. The time constant t_0 was estimated individually for each mouse from the kidney data. Data fitting was done using Levenberg-Marquardt nonlinear least squares procedure. Parametric images were computed and only the statistically significant parameter estimates were displayed. Statistical significance for both D_0 and D_1, or only for D_1, identified "perfused" voxels that displayed the typical signal curve enhancement on injection of the contrast agent injection.

IFP Measurement

IFP was measured using a "wick-in-needle" apparatus (30). An 18-gauge needle with a 1-mm side hole located at about 5 mm from the needle tip was connected to a pressure monitor system (295-1 Pressure, Stryker, Brussels, Belgium) specially designed for measuring tissue fluid pressures. The system was filled with saline water. A zero reference for the pressure system was done before each experiment and was reset by placing the needle beside the tumor. The skin was depilated the day before the experiment. Measurements were done by inserting the needle into the center of the tumor and injecting 50 μL of 0.9% sodium chloride to ensure fluid communication between the tumor and the pressure monitor system. During injection, the pressure rose by 30 to 50 mm Hg and rapidly decreased to a stable value. If the pressure remained elevated, rapidly dropped, or fluctuated, the value was discarded. Measurements were carried out after 2 days of treatment with thalidomide or vehicle. Acute nicotinamide delivery (500 mg/kg i.p. 120 minutes before the experiment) was used as a positive control (31).

Immunohistochemistry

FSAII tumor–bearing mice were sacrificed after 2 days of treatment with thalidomide (200 mg/kg) or vehicle. Tumor cryoslices were immunoprobed with rat monoclonal CD31 IgG2a antibodies (PharMingen, San Diego, CA). Rabbit polyclonal anti-rat IgG peroxidase-conjugated antibodies (Jackson ImmunoResearch Laboratories, West Grove, PA) and AEC substrate system (DakoCytomation, Heverlee, Belgium) were used for revelation; sections were finally counterstained with Mayer's hematoxylin.

Irradiation and Tumor Regrowth Delay Assay

The tumor-bearing leg was locally irradiated with 20 Gy of 250-kV X-rays (RT 250, Philips Medical Systems, Hamburg, Germany). The tumor was centered in a 3-cm-diameter circular irradiation field. Different irradiation protocols were done: a single-dose irradiation of 20 Gy after intratumoral injection, a single-dose irradiation of 20 Gy after 2 days of treatment (i.p.), a single-dose irradiation of 20 Gy after 4 days of treatment (i.p.), and a single dose of 20 Gy followed by 2 days of treatment (i.p.). In each experiment, the treated group was compared with groups of mice receiving the vehicle (DMSO) alone, and DMSO + X-rays (RX). After treatment, tumor growth was determined daily by measuring transversal and anteroposterior tumor diameters until they reached a diameter of 16 mm, at which time the mice were sacrificed. A linear fit was obtained between 8 and 16 mm, which allowed us to determine the time to reach a particular size for each mouse.

Tumor Cell Culture

FSAII tumors in mice were dissected in a sterile environment and gently pieced in McCoy's medium. The cell suspension was filtered (100-μm pore size nylon filter, Millipore, Brussels, Belgium), centrifuged (5 minutes, 450 × *g*, 4°C), and cells were set to culture in DMEM containing 10% fetal bovine serum. Confluent cells were treated with thalidomide (100 μmol/L) or vehicle (DMSO) 1 hour before being irradiated at 2 Gy. To assess the cell radiosensitivity, trypan blue exclusion dye method and a clonogenic cell survival assay were done. For the former, the cells were counted for viability 24 hours after irradiation. For the latter, the cells were washed and reincubated in the conditioned medium without drug 24 hours after irradiation. After a 7-day incubation in a humidified 5% CO_2 atmosphere at 37°C, the dishes were stained with crystal violet and colonies with >50 cells were counted.

Statistical Analysis

Results are given as means ± SE values from *n* animals. Comparisons between groups were made with Student's two-tailed *t* test and a *P* value <0.05 was considered significant. The GraphPad Prism 4.0 software was used for statistical analysis.

RESULTS

Effect of Thalidomide on Tumor Oxygenation

EPR oximetry relies on the oxygen-dependent broadening of the EPR line width of a paramagnetic oxygen sensor implanted in the tumor (25). This technique is designed for

continuous measurement of the local pO_2 without altering the local oxygen concentration, and allows repeated measurements from the same site over long periods of time. Mice were randomized according to the initial pO_2 observed on day 0 (before any treatment): thalidomide, 3.9 ± 1.3 mm Hg (n = 8); control groups, 4.1 ± 1.7 mm Hg (n = 5). Daily thalidomide treatment modified the tumor pO_2 (Fig. 1). For the thalidomide group, a significant increase ($P < 0.05$) was observed after 2 days of treatment (day 2) with a maximum value of 15.5 ± 4.6 mm Hg (mean ± SE), followed by continuous decrease in pO_2. The amount of increase in pO_2 was quite variable from one tumor to another. However, the time of maximal increase was the same for 6 of 8 mice. Two mice had their maximal increase on day 3. No such increase was observed for the control group: the value of pO_2 remained relatively stable (Fig. 1). The tumor pO_2 was found to be statistically different between thalidomide and control groups at days 2 and 3 ($P < 0.05$). Tumor perfusion, IFP, and the tumor regrowth delay experiments were then done on day 2, when the maximal increase in pO_2 was observed.

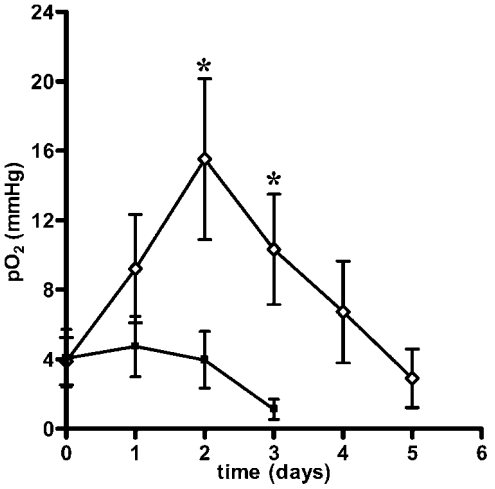

Fig. 1 Effect of daily thalidomide treatment on FSAII tumor pO_2 monitored by EPR oximetry. ■, control group (n = 5); ◇, thalidomide group (n = 8). Note the significant increase in pO_2 at days 2 and 3 (*, $P < 0.05$) for treated group. *Points,* mean; *bars,* SE.

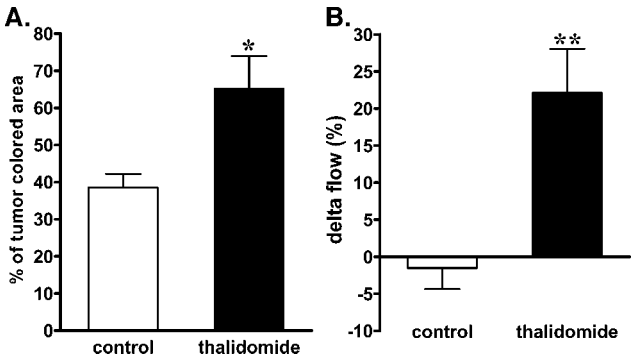

Fig. 2 *A*, effect of 2 days of thalidomide treatment on tumor perfusion assessed by Patent Blue staining. *Columns,* mean value of tumor percentage of colored area for control group (n = 5) and thalidomide group (n = 4); *bars,* SE. An increase of 70% is observed for the treated group (*P, < 0.05). *B,* effect of 2 days of thalidomide treatment on tumor perfusion assessed by laser Doppler imaging. *Columns,* tumor change in flow (%) for the control group (n = 8) and thalidomide group (n = 6) compared with the flow measured before initiating the treatment; *bars,* SE. Note the significant increase in superficial blood flow (**, $P < 0.01$).

Effects of Thalidomide on Tumor Perfusion

Three techniques were used to estimate the blood flow inside the tumor.

Patent Blue Staining. A rough estimate of the tumor perfusion was carried out using the colored area observed in tumors after injection of a dye. Tumors with thalidomide treatment stained more positive (n = 4; 65.3 ± 8.7%) than tumors treated with vehicle (n = 5; 38.4 ± 3.7%; Fig. 2*A*). This difference was found to be statistically significant ($P < 0.05$).

Laser Doppler Imaging. Laser Doppler imaging was used to assess the superficial tumor blood flow. This technique allows the perfusion measurement to be done on the same mouse over the time of treatment. All the tumors in treated mice (n = 6) showed an increase in perfusion after 2 days of thalidomide treatment compared with their initial perfusion value ($P < 0.01$). The mean increase for the thalidomide-treated group was 22.1 ± 5.9% (Fig. 2*B*). For each treated mouse, the analysis of the histogram of the pixel distribution as a function of the flow showed an increase in the number of pixels showing a higher flow. No significant flow modification was observed for the mice treated with vehicle alone (n = 8).

Dynamic Contrast-Enhanced MRI. DCE-MRI was done to evaluate D_0, D_1, and K_2 pharmacokinetic parameters in significantly enhancing voxels as determined by the cluster analysis. To take into account the maximal plasma P792 concentration (A_0), the D_0 and D_1 values were divided by A_0. Results are summarized in Fig. 3. The plasma volume fraction was significantly higher in the thalidomide group (n = 5) compared with the control mice (n = 4; $P < 0.01$). D_1/A_0, corresponding to the product of the volume fraction of extravascular extracellular space and the leakage rate, was higher in the thalidomide group than the control group, but this difference was not statistically significant ($P > 0.05$). The fractional efflux rate from interstitial space back to plasma (K_2) was uniformly low in the control group in comparison with the thalidomide group ($P < 0.05$).

Effect of Thalidomide on IFP

Tumor IFP measurements were done in both control and thalidomide groups after 2 days of treatment. We observed a significant decrease ($P < 0.01$) in tumor IFP between control (n = 7) and thalidomide (n = 10) groups with values of 19 ± 0.6 and 15 ± 0.9 mm Hg, respectively. Acute nicotinamide injection (a positive control) induced a tumor IFP decrease of approximately 25%, which is consistent with previous observations (31).

Histologic Analysis

Immunohistologic staining with antibody directed against CD31 was used to investigate whether the tumor vascularization and organization were modified 2 days after thalidomide treatment. The examination of histologic sections by independent observers indicated that tumors were heterogeneous in their microvascular density. Vessels were uniformly distributed throughout the tumor for the control group compared with the

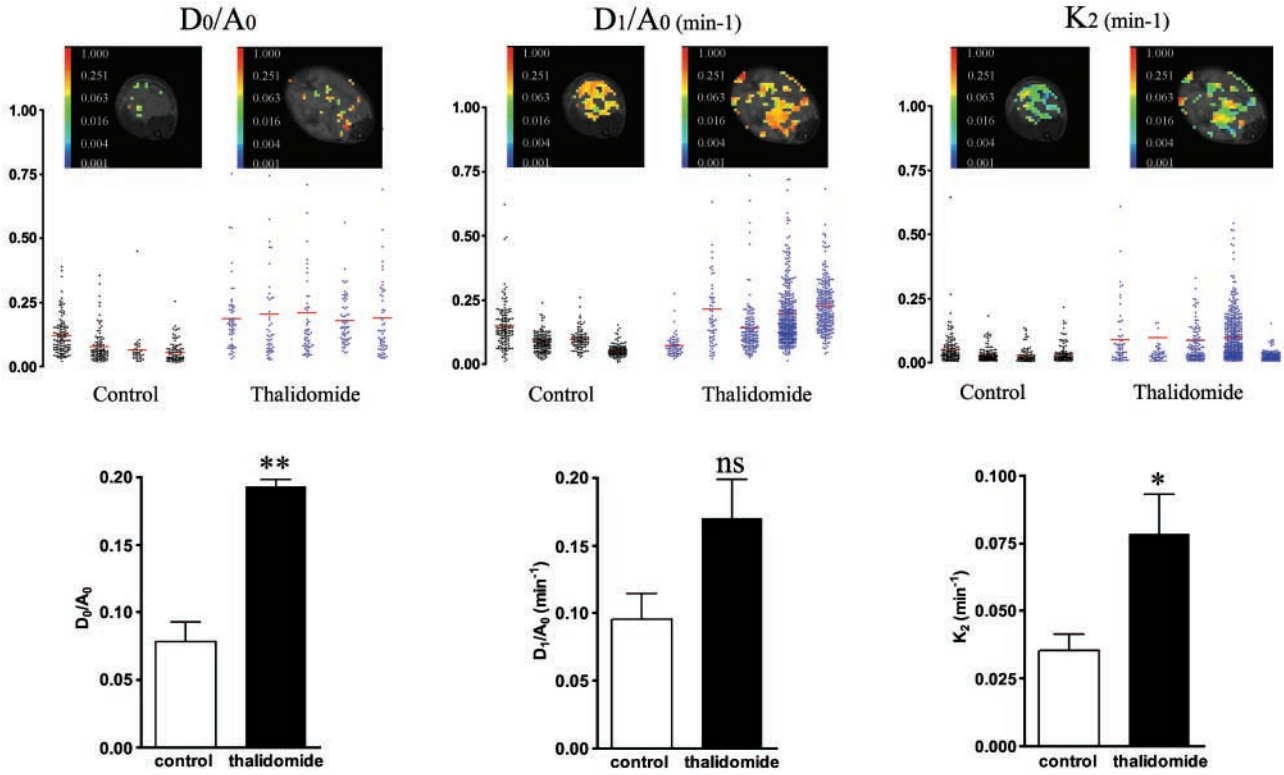

Fig. 3 Effect of 2 days' thalidomide treatment on the DCE-MRI pharmacokinetic parameters. *Top,* typical parametric MRI images of FSAII tumors after treatment with thalidomide or vehicle (*Control*). *Middle,* distribution of pharmacokinetics parameters in individual tumors treated with vehicle (n = 4) or thalidomide (n = 5). D_0/A_0 is the plasma volume fraction, D_1/A_0 corresponds to the product of the volume fraction of the extravascular extracellular space and the leakage rate, and K_2 is the fractional rate of efflux from interstitial space back to the plasma. In the distribution graph, the line represents the mean of each parameter for the individual mouse. *Bottom,* overall estimation of pharmacokinetic parameters after thalidomide treatment. Columns, mean of the values pooled from individual tumors; *bars,* SEM. *, $P < 0.05$; **, $P < 0.01$. *NS,* not significant.

treated group in which they were preferentially localized at the margin of the tumor with diameters substantially increased (Fig. 4). A decrease in the number of small vessels was also observed. Necrosis was present in both groups. Unexpectedly, thalidomide also modified tumor architecture, promoting heaps of tumor cells instead of being randomly distributed (Fig. 4).

Effect of Thalidomide on the FSAII Tumor Regrowth Delay

Without irradiation, no significant difference was observed concerning the regrowth delay for thalidomide (n = 5) and control groups (n = 7; not shown). The regrowth delay (days) between control + RX and thalidomide + RX was -0.8 ± 0.7, -0.4 ± 1.2, -1.0 ± 0.7, and 1.8 ± 0.7 for intratumoral treatment just before RX, RX followed by 2 days of treatment, 4 days of treatment followed by RX, and 2 days of treatment followed by RX, respectively (Table 1). Thalidomide treatment significantly increased the tumor regrowth delay when applied during 2 days before the irradiation (1.4-fold increase). In this case, the time to reach a 12-mm tumor diameter was 5.2 ± 0.3 days for nonirradiated mice (n = 5), 10.3 ± 0.6 days for vehicle and RX (n = 5), and 12.1 ± 0.5 days for thalidomide and RX (n = 5). In other protocols, there was no significant change in the sensitivity of tumor to irradiation, indicating no benefit for the combination of thalidomide with radiotherapy.

Effect of Thalidomide on the Radiosensitivity of FSAII Cells *In vitro*

To discriminate between an oxygen effect and a direct radiosensitizing effect, the radiosensitivity was tested on FSAII cells in the presence of thalidomide. A 2-Gy irradiation led to a 55% cell death. Compared to control cells, a 100-μmol/L concentration of thalidomide did not exert any sensitizing effect regardless of whether trypan blue exclusion dye method or clonogenic cell survival assay was used. This concentration is higher than the concentration reachable in tumors and is never achieved in patient plasma (32).

DISCUSSION

To improve existing therapies such as chemotherapy or radiotherapy, or to develop new treatment strategies, it is essential to know how the tumor microenvironment changes in response to tumor therapies. Given that antiangiogenic agents will likely be combined with radiation therapy, it is critical to understand alterations in tumor oxygenation and perfusion, as well as to define optimal time points for the delivery of radiation. Up until this time, the evolution of the tumor microenvironment after thalidomide treatment had not been thoroughly studied. The purpose of the present work was to

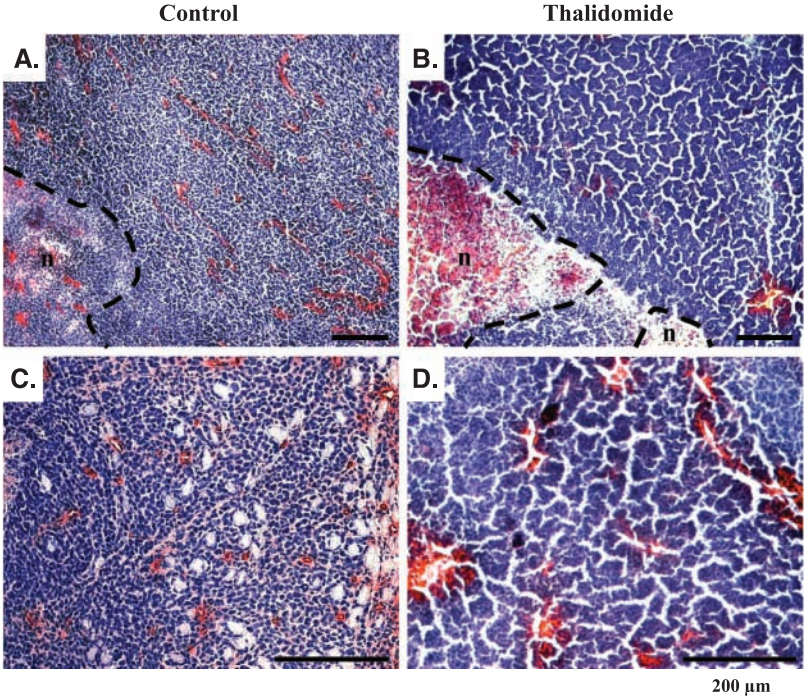

Fig. 4 Typical histologic sections of FSAII tumor after 2 days of treatment with thalidomide or vehicle. Immunohistologic staining was carried out with antibody against CD31. *A* and *B,* center of the tumor; *C* and *D,* tumor margin. For the control group, the vessels are evenly distributed throughout the tumor even in the center compared with treated group in which the vessels are preferentially localized at the margin. Treated tumors present a decrease in the amount of small vessels; the remaining ones are large. Thalidomide also promotes heaps of tumor cells instead of being randomly distributed. *n,* necrosis.

measure the modifications in the tumor environment early after an antiangiogenic treatment of thalidomide, with a special focus on possible normalization of the tumor vasculature (7, 8) that could be beneficial for radiotherapy.

Our results showed an increase in tumor pO_2 during the first 2 days of thalidomide treatment (Fig. 1) followed by a decrease in pO_2. Such an increase in oxygen levels after antiangiogenic treatment had previously been reported by Lee et al. (12), Fenton et al. (33), and Teicher et al. (34–36). However, no oxygenation kinetic analysis was done in those studies. The decrease in tumor pO_2 that we observed could be the result either of the antiangiogenic effect of thalidomide or a decrease in oxygen tension due to the tumor growth (11) as seen for the control group. Our observation of increased tumor oxygenation is likely the result of the ability of thalidomide to modify tumor microenvironment parameters such as the vascular supply and tumor perfusion. It has been shown that a short-term administration of antiangiogenic agents could prune inefficient vascular sprouts (8), leading to the establishment of more efficient flow paths. In fact, previous work has shown an increase in tumor oxygenation after antiangiogenic treatment despite a reduction in vascular density, indicating that the quality of vascular organization rather than the quantity of vessels determine tumor pO_2 (12). This vascular stabilization could improve vascular function in the short term (8). Our histologic analysis reveals profound modifications in the vascular supply: a reduction in the number of tumor microvessels after thalidomide treatment together with a dilation of the remaining vessels with no decrease in the tumor vascular density (Fig. 4). The perfusion measured by DCE-MRI showed an increased plasma volume fraction (Fig. 3). This could be explained by the shift to larger blood vessel diameters as observed in histology analysis, perhaps due to compensation for the loss of small vessels (37). Patent Blue staining and laser Doppler imaging also showed an increase in tumor blood flow (Fig. 2*A* and *B*). The decrease in the tumor IFP could also explain the increase in perfusion and oxygenation by a mechanical effect: as the IFP decreases, there could be less pressure on tumor blood vessel walls, resulting in an increase in vascular diameter due to capillary compliance and lower geometric vascular resistance (38). As mentioned above, short-term administration of thalidomide induced a lowering of tumor IFP, probably resulting from the suppression of tumor immature blood vessels and from interstitial matrix remodeling. This decrease in IFP will then enhance transcapillary transport into the tumor interstitium because the interstitial pressure participates in the control of transcapillary fluid fluxes (8,39,40). DCE-MRI values of D_1/A_0 and and K_2, which reflect transcapillary flux, confirmed the increase in fluid flux into the tumor and into the vessel for the thalidomide group (Fig. 3).

The radiotherapy experiments showed the need to monitor the tumor microenvironment before planning combinations of treatments. In fact, thalidomide increased the radiosensitivity of FSAII tumor only after 2 days of treatment (Table 1). The other time windows showed no benefits. The radiosensitizing property of thalidomide can be attributed to the local increase in vascular supply of O_2, as shown by EPR oximetry, because tumor cell cultures with thalidomide were not radiosensitized. These results are consistent with those obtained by Kinuya et al. (41) on other tumor cell types. Therefore, the regrowth delay observed is only due to the oxygen effect. An improvement in response to irradiation when antiangiogenic treatment is given has already been reported (12, 15–17, 35, 42–43). However, in those studies, the increase in tumor oxygenation induced by antiangiogenic agents was not always reported as the cause of the radioresponse

Table 1 Irradiation experiments

	Time to reach 12 mm (d)	Regrowth delay (d)	Change (days) between control + RX and thalidomide + RX
Intratumoral treatment just before RX			
Nonirradiated control (n = 7)	4.5 ± 0.3		
Control + RX (n = 5)	8.8 ± 0.4	+4.3 ± 0.5	
Thalidomide + RX (n = 5)	8.0 ± 0.5	+3.5 ± 0.6	−0.8 ± 0.7 NS
RX followed by 2 days of treatment			
Nonirradiated control (n = 7)	4.5 ± 0.3		
Control + RX (n = 4)	10.1 ± 1.10	+5.6 ± 0.9	
Thalidomide + RX (n = 4)	9.7 ± 0.5	+5.2 ± 0.6	−0.4 ± 1.2 NS
Four days treatment followed by RX			
Nonirradiated control (n = 8)	5.5 ± 0.5		
Control + RX (n = 4)	10.1 ± 0.6	+4.6 ± 0.8	
Thalidomide + RX (n = 4)	9.1 ± 0.3	+3.6 ± 0.7	−1.0 ± 0.7 NS
Two days treatment followed by RX			
Nonirradiated control (n = 5)	5.2 ± 0.3		
Control + RX (n = 5)	10.3 ± 0.6	+5.1 ± 0.6	
Thalidomide + RX (n = 5)	12.1 ± 0.5	+6.9 ± 0.6	1.8 ± 0.7*

NOTE. Data are mean ± SE.
Abbreviation: *NS,* not significant.
*P < 0.05.

improvement. Our study showed that short-term thalidomide treatment before irradiation can improve vascular efficacy and oxygenation, which is the cause of the tumor regrowth delay observed. No effect of thalidomide alone on FSAII cell growth was observed (results not shown). This is consistent with previous *in vitro* experiments, which showed that thalidomide was unable to reduce proliferation of glioma cells (44) and was unable to exert direct cytotoxicity on LS180 cells (41). Moreover, no difference was observed between the tumor growth in control and thalidomide-treated mice. This failure to inhibit tumor growth has also been shown in other studies (45–47).

In conclusion, the study of changes in the tumor microenvironment during antiangiogenic drug treatment is of crucial importance for planning the combination of such drugs with radiation therapy. Our study reveals a short-term increase in tumor blood flow after thalidomide treatment. This could result, at least in part, from the normalization of tumor immature blood vessels. This normalization of the tumor vasculature decreased the tumor blood vessel resistance and tumor IFP. Consequently, the tumor pO_2 was increased at the early phase of the thalidomide treatment. When irradiated at the time for which the maximal pO2 was observed, a radiosensitization was observed.

ACKNOWLEDGMENTS

We thank Guerbet Laboratories (Roissy, France) for providing P792.

REFERENCES

1. Carmeliet P, Jain RK. Angiogenesis in cancer and other diseases. Nature 2000;407:249–57.

2. Papetti M, Herman IM. Mechanisms of normal and tumor-derived angiogenesis. Am J Physiol Cell Physiol 2002;282:C947–70.

3. Konerding MA, Van Ackern C, Fait E, Steinberg F, Streffer C. Morphological aspects of tumor angiogenesis and microcirculation. In: Molls M, Vaupels P, editors. Blood perfusion and microenvironment of human tumors. Berlin: Springer-Verlag; 1998. p. 5–17.

4. Munn LL. Aberrant vascular architecture in tumors and its importance in drug-based therapies. Drug Discov Today 2003;8:396–403.

5. Dewhirst MW, Kimura H, Rehmus SW, et al. Microvascular studies on the origins of perfusion-limited hypoxia. Br J Cancer Suppl 1996;27:247–51.

6. Burke PA, DeNardo SJ. Antiangiogenic agents and their promising potential in combined therapy. Crit Rev Oncol Hematol 2001;39:155–71.

7. Jain RK. Normalizing tumor vasculature with anti-angiogenic therapy: a new paradigm for combination therapy. Nat Med 2001;7:987–9.

8. Tong RT, Boucher Y, Kozin SV, Winkler F, Hicklin DJ, Jain RK. Vascular normalization by vascular endothelial growth factor receptor 2 blockade induces a pressure gradient across the vasculature and improves drug penetration in tumors. Cancer Res 2004;64:3731–6.

9. Tzuzuki Y, Fukumura D, Oosthuyse B, Koike C, Carmeliet P, Jain RK. VEGF modulation by targeting HIF-1α > HRE > VEGF cascade differentially regulates vascular response and growth rate in tumors. Cancer Res 2000;60:6248–52.

10. Kadambi A, Carreira CM, Yun C, et al. Vascular endothelial growth factor (VEGF)-C differentially affects tumor vascular function and leukocyte recruitment. Cancer Res 2001;61:2404–8.

11. Hansen-Algenstaedt N, Stoll BR, Padera TP, et al. Tumor oxygenation in hormone-dependent tumors during vascular endothelial growth factor receptor-2 blockade, hormone ablation, and chemotherapy. Cancer Res 2000;60:4556–60.

12. Lee C, Heijn M, Di Tomaso E, et al. Anti-vascular endothelial growth factor treatment augments tumor radiation response under normoxic or hypoxic conditions. Cancer Res 2000;60:5565–70.

13. Bello L, Carrabba G, Giussani C, et al. A. Low-dose chemotherapy combined with an antiangiogenic drug reduces human glioma growth *in vivo*. Cancer Res 2001;61:7501–6.

14. Shalinsky DR, Brekken J, Zou H, et al. Marked antiangiogenic and antitumor efficacy of AG3340 in chemoresistant human non-small cancer lung cancer tumors: single agent and combination chemotherapy studies. Clin Cancer Res 1999;5:1905–17.

15. Mauceri HJ, Hanna NN, Beckett MA, et al. Combined effect of angiostatin and ionizing radiation in antitumour therapy. Nature 1998;394:287–91.

16. Gorski DH, Mauceri HJ, Salloum RM, et al. Potentiation of the antitumor effect of ionizing radiation by brief concomitant exposures to angiostatin. Cancer Res 1998;58:5686–9.

17. Gorski DH, Beckett MA, Jaskowiak NT, et al. Blockade of the vascular endothelial growth factor stress response increases the antitumor effects of ionizing radiation. Cancer Res 1999;59:3374–8.

18. D'Amato RJ, Loughnan MS, Flynn E, Folkman J. Thalidomide is an inhibitor of angiogenesis. Proc Natl Acad Sci U S A 1994;91:4082–5.

19. Kenyon BM, Browne F, D'Amato RJ. Effects of thalidomide and related metabolites in mouse corneal model of neovascularization. Exp Eye Res 1997;64:971–8.

20. Kruse FE, Joussen AM, Rohrschneider K, Becker MD, Völcker HE. Thalidomide inhibits corneal angiogenesis induced by vascular

endothelial growth factor. Graefes Arch Clin Exp Ophthalmol 1998; 236:461–6.

21. Verheul HMW, Panigrahy D, Yuan J, D'Amato RJ. Combination oral antiangiogenic therapy with thalidomide and sulindac inhibits tumour growth in rabbits. Br J Cancer 1999;79:114–8.

22. Von Moos R, Stolz R, Cerny T, Gillessen S. Thalidomide: from tragedy to promise. Swiss Med Wkly 2003;133:77–87.

23. Volpe JP, Hunter N, Basic I, Milas L. Metastatic properties of murine sarcomas and carcinomas. I. Positive correlation with lung colonization and lack of correlation with s.c. tumor take. Clin Exp Metastasis 1985; 3:281–94.

24. Jordan BF, Baudelet C, Gallez B. Carbon-centered radicals as oxygen sensors for *in vivo* electron paramagnetic resonance: screening for an optimal probe among commercially available charcoals. Magn Reson Mater Phys Med Biol 1998;7:121–9.

25. Gallez B, Jordan BF, Baudelet C, Misson PD. Pharmacological modifications of the partial pressure of oxygen in murine tumors: evaluation using *in vivo* EPR oximetry. Magn Reson Med 1999;42: 627–30.

26. Jordan BF, Misson P, Demeure R, Baudelet C, Beghein N, Gallez B. Changes in tumor oxygenation/perfusion induced by the NO donor, isosorbide dinitrate, in comparison with carbogen: monitoring by EPR and MRI. Int J Radiat Oncol Biol Phys 2000; 48:565–70.

27. Sersa G, Cemazar M, Miklavcic D, Chaplin, DJ. Tumor blood flow modifying effect of electrochemotherapy with bleomycin. Anticancer Res 1999;19:4017–22.

28. Baudelet C, Gallez B. Cluster analysis of BOLD fMRI time series in tumors to study the heterogeneity of hemodynamic response to treatment. Magn Reson Med 2003;49:985–90.

29. Su MY, Jao JC, Nalcioglu O. Measurement of vascular volume fraction and blood-tissue permeability constants with a pharmacokinetic model: studies in rat muscle tumors with dynamic Gd-DTPA enhanced MRI. Magn Reson Med 1994;32:714–24.

30. Boucher Y, Kirkwood JM, Opacic D, Desantis M, Jain RK. Interstitial hypertension in superficial metastatic melanomas in humans. Cancer Res 1991;51:6691–4.

31. Lee I, Boucher Y, Jain RK. Nicotinamide can lower tumor interstitial fluid pressure: mechanistic and therapeutic implications. Cancer Res 1992;52:3237–40.

32. Lentzsch S, LeBlanc R, Podar K, et al. Immunomodulatory analogs of thalidomide inhibit growth of HS Sultan cells and angiogenesis *in vivo*. Leukemia 2003;17:41–4.

33. Fenton BM, Paoni SF, Grimwood BG, Ding I. Disparate effects of endostatin on tumor vascular perfusion and hypoxia in two murine mammary carcinomas. Int J Radiat Oncol Biol Phys 2003;57: 1038–46.

34. Teicher BA, Holden SA, Ara G, et al. Influence of an anti-angiogenic treatment on 9L gliosarcoma: oxygenation and response to cytotoxic therapy. Int J Cancer 1995;61:732–7.

35. Teicher BA, Dupis N, Kusomoto T, et al. Anti-angiogenic agents can increase tumor oxygenation and response to radiation therapy. Radiat Oncol Investig 1995;2:269–76.

36. Teicher BA, Williams JI, Takeuchi H, Ara G, Herbst RS, Buxton D. Potential of the aminosterol, squalamine in combination therapy in the rat 13762 mammary carcinoma and the murine Lewis lung carcinoma. Anticancer Res 1998;18:2567–73.

37. Drevs J, Muller-Driver R, Wittig C, et al. PTK787/ZK 222584, a specific vascular endothelial growth factor-receptor tyrosine kinase inhibitor, affects the anatomy of the tumor vascular bed and the functional vascular properties as detected by dynamic enhanced magnetic resonance imaging. Cancer Res 2002;62:4015–22.

38. Milosevic MF, Fyles AW, Hill RP. The relationship between elevated interstitial fluid pressure and blood flow in tumors: a bioengineering analysis. Int J Radiat Oncol Biol Phys 1999;43:1111–23.

39. Aukland K, Reed RK. Interstitial-lymphatic mechanisms in the control of extracellular fluid volume. Physiol Rev 1993;73:1–78.

40. Rubin K, Sjoquist M, Gustafsson AM, Isaksson B, Salvessen G, Reed RK. Lowering of tumoral interstitial fluid pressure by prostaglandin E(1) is paralleled by an increased uptake of ^{51}Cr-EDTA. Int J Cancer 2000;86:636–43.

41. Kinuya S, Kawashima A, Yokoyama K, et al. Cooperative effect of radioimmunotherapy and antiangiogenic therapy with thalidomide in human cancer xenografts. J Nucl Med 2002;43:1084–9.

42. Lund EL, Bastholm L, Kristjansen PE. Therapeutic synergy of TNP-470 and ionizing radiation: effects on tumor growth, vessel morphology, and angiogenesis in human glioblastoma multiforme xenografts. Clin Cancer Res 2000;6:971–8.

43. Kozin SV, Boucher Y, Hicklin DJ, Bohlen P, Jain RK, Suit HD. Vascular endothelial growth factor receptor-2-blocking antibody potentiates radiation-induced long-term control of human tumor xenografts. Cancer Res 2001;61:39–44.

44. Moreira AL, Friedlander DR, Shif B, Kaplan G, Zagzag D. Thalidomide and a thalidomide analogue inhibit endothelial cell proliferation *in vitro*. J Neurooncol 1999;43:109–14.

45. Gutman M, Szold A, Ravid A, Lazauskas T, Merimsky O, Klausner JM. Failure of thalidomide to inhibit tumor growth and angiogenesis *in vivo*. Anticancer Res 1996;16:3673–7.

46. Minchinton AI, Fryer KH, Wendt KR, Clow KA, Hayes MM. The effect of thalidomide on experimental tumors and metastases. Anticancer Drugs 1996;7:339–43.

47. Belo AV, Ferreira MA, Bosco AA, Machado RD, Andrade SP. Differential effects of thalidomide on angiogenesis and tumor growth in mice. Inflammation 2001;25:91–6.